

## ADVANCED PIECEWISE-HARMONIC-BALANCE NOISE ANALYSIS OF NONLINEAR MICROWAVE CIRCUITS WITH APPLICATION TO SCHOTTKY-BARRIER DIODES

Vittorio RIZZOLI (1), Franco MASTRI (2), and Diego MASOTTI (3)

(1) Dipartimento di Elettronica, Informatica e Sistemistica, University of Bologna

(2) Istituto di Elettrotecnica, University of Bologna

(3) Fondazione Guglielmo Marconi

Villa Griffone, 40044 Pontecchio Marconi, Bologna - ITALY

### ABSTRACT

The paper introduces a number of significant advances in harmonic-balance noise analysis algorithms, and discusses their incorporation in a general-purpose nonlinear circuit simulator. The new capabilities allow for the first time the implementation of a full noise model of the Schottky diode, including the excess noise produced by hot electron generation, intervalley scattering, and trapping effects, and accounting for the series resistance nonlinearity.

### INTRODUCTION

Noise analysis is one of the indispensable capabilities of a modern general-purpose simulator for nonlinear microwave circuits. Partial solutions of this problem have been presented by several authors (e.g., [1 - 3]), but only recently truly general frequency-domain formulations based on the piecewise [4] and on the nodal [5] harmonic-balance (HB) method have began to appear. However, the noise analysis techniques described in these works still have a number of significant limitations which are effectively overcome by the advanced analysis method described in this paper.

Let the circuit be subdivided into a linear and a nonlinear subnetwork connected through a number  $n_D$  of ports. The nonlinear subnetwork is replaced by a noise-free nonlinear multiport with a noise current source  $j_m(t)$  and a noise voltage source  $u_m(t)$  (*nonlinear noise sources*) connected with each port ( $1 \leq m \leq n_D$ ). The simultaneous consideration of both kinds of sources is necessary in many situations, including diodes with a nonlinear series resistance and bipolar transistors with a nonlinear base resistance. With the nodal approach, series sources can be included by replacing the conventional nodal method with a modified nodal analysis [5], but this implies a considerable size increase of the Jacobian matrix, especially for large circuits. The piecewise technique can deal with noise voltage sources in closed form without requiring any size increase of the matrices to be handled. In the present work, this result is obtained by formally extending the analysis of [4] to include noise voltage sources.

When the nonlinear circuit is pumped by an external sinusoidal signal such as the local oscillator for a mixer, the nonlinear noise sources are modulated by the steady-state regime, which produces correlations among the noise source sidebands [1, 4]. In previous work, this problem has been solved by introducing frequency-independent modulating functions in the dynamic expressions of the nonlinear noise sources [4, 5]. This approximation is not acceptable in a number of interesting situations, such as for intrinsic FETs with a nonlinear feedback capacitance and/or with frequency-dependent foundry factors [6]. A significant advance introduced by this paper is the ability to account for frequency-sensitive modulation of the nonlinear noise source sidebands. Also, the application of the modulation concept to sets of partially

correlated noise sources is revised and more correctly restated.

As an important application, it is shown that these new capabilities allow for the first time a full noise model of the Schottky-barrier diode to be implemented in a general-purpose simulation program. The model takes into account the shot noise, the conventional thermal noise, and the excess noise produced by hot electron generation, intervalley scattering, and trapping effects [7]. The dependence of all the noise sources on the depletion layer thickness, as well as the nonlinearity of the diode series resistance, are exactly accounted for. It is shown that the new algorithms provide a straightforward closed-form solution to this difficult and as yet unsolved problem. Computations of the noise temperature of a millimeter-wave diode mixer are presented for illustrative purposes, and the high numerical efficiency of the noise analysis technique is demonstrated.

### THE ANALYSIS ALGORITHM

Let the nonlinear circuit be pumped by a large sinusoidal signal of angular frequency  $\omega_0$  (*carrier*) superimposed on the noise sources. We assume that the noise signals are so small that their intermodulation (IM) products can be neglected. Thus the electrical regime only contains carrier harmonics and carrier-to-noise IM products which are first-order in the noise components (*noise sidebands*). In this way a broadband noise analysis is reduced to a sequence of independent spot noise analyses. For each of these, a generic noise waveform is an infinite family of pseudosinusoids having random amplitudes and phases [1], located at the noise sidebands corresponding to a given deviation  $\omega$  from the carrier. The mathematical representation of such a waveform is

$$\begin{aligned} \delta n(t, \omega) &= \sum_k \delta n_k(t, \omega) = \\ &= \sqrt{2} \sum_k \delta N_k(\omega) \exp[j(\omega + k\omega_0)t] \end{aligned} \quad (1)$$

where  $\langle |\delta N_k(\omega)|^2 \rangle$  represents the expected mean-square value of the  $k$ -th sideband components ( $\langle \rangle$  denotes the statistical mean or ensemble average).

The analysis approach is an extension of the method discussed in [4]. The unperturbed (noiseless) steady-state regime is first determined by the piecewise HB technique. The nonlinear subnetwork is then replaced by a multifrequency linear multiport described by the admittance conversion matrix evaluated in the neighborhood of the steady state. Making use of the linearized equations of the nonlinear subnetwork and of the conventional frequency-domain equations of the linear subnetwork, two families of sideband-to-sideband conversion matrices are derived by standard linear circuit techniques.

IF1

Specifically, the conversion matrix mapping the p-th sideband of the noise current (respectively, voltage) sources onto the k-th sideband of the load noise current is denoted by  $T_{kp}^J$  (respectively,  $T_{kp}^U$ ). The noise power delivered to a load  $R$  in a narrow frequency band  $\Delta\omega$  in the neighborhood of  $\omega + k\omega_0$  is then given by

$$dN_k(\omega) = R \sum_p T_{kp}^J \mathbb{C}_L(\omega + p\omega_0) T_{kp}^{J*} \quad (2)$$

$$dN_k(\omega) = R \sum_{p,q} \left\{ T_{kp}^U \langle U_p(\omega) U_q^*(\omega) \rangle T_{kq}^{U*} + T_{kp}^J \langle J_p(\omega) J_q^*(\omega) \rangle T_{kq}^{J*} + 2\operatorname{Re} \left[ T_{kp}^U \langle U_p(\omega) J_q^*(\omega) \rangle T_{kq}^{J*} \right] \right\} \quad (3)$$

for the contributions of the linear and nonlinear noise sources, respectively (the symbol  $*$  denotes the conjugate transposed of a complex matrix). In (2)  $\mathbb{C}_L(\omega)$  is the correlation matrix of the Norton equivalent noise sources of the linear subnetwork.  $\mathbb{C}_L(\omega)$  is a known function of the linear subnetwork topology and temperature [8]. Note that for the computation of the term of (2) having  $p = k$ , the linear subnetwork must be augmented of an additional port obtained by cutting the load branch.

#### MODULATION OF THE NONLINEAR NOISE SOURCES

In most practical cases, the nonlinear noise sources arise from the superposition of noise contributions generated by several independent physical mechanisms. This may be true even for a single nonlinear device: for instance, a diode will generate shot noise in the junction and thermal noise in the series resistance. Keeping this in mind, we introduce the following decomposition of the nonlinear noise sources:

$$U = \sum_i U^{(i)} \quad J = \sum_i J^{(i)} \quad (4)$$

where each superscript  $i$  is associated with an independent mechanism of noise generation. The noise voltage and current sources having the same superscript  $i$  in (4) are fully correlated, and their effects are described by a summation of the form (3). On the other hand, noise sources having different physical origins are not correlated, and their effects are superimposed in power. Thus, to compute the overall load noise we have to add a contribution of the form (3) for each independent set of fully correlated sources. The following discussion refers to any such set of sources; the superscript  $i$  is understood for simplicity.

When the circuit is pumped by a large sinusoidal signal, the nonlinear noise sources are periodically modulated, and the modulation process can be analyzed by a quasi-stationary assumption [1, 4]. For the time-domain waveforms, this approximation is interpreted by introducing in (1) a deterministic modulating function for each sideband. For the noise voltage sources (e.g.) we thus obtain the following time- and frequency-domain representations

$$u(t, \omega) = \sum_k h_k^U(t, \omega) u_{DCk}(t, \omega) \quad (5)$$

$$U_p(\omega) = \sum_k H_{k,p-k}^U(\omega) U_{DCk}(\omega)$$

where the subscript DC denotes static conditions (DC bias only). In (5)  $h_k^U(t, \omega)$  is a diagonal matrix of modulating functions  $h_{k,m}^U(t, \omega)$  ( $1 \leq m \leq n_D$ ), and  $H_{k,s}^U(\omega)$  is the diagonal matrix of their s-th harmonics. Now let the unperturbed steady state be denoted by  $x_{ss}(t)$ , where  $x(t)$  is a vector of time-dependent state variables. The DC component of  $x_{ss}(t)$ , namely  $X_0$ , represents the bias point. The spectral density of the m-th noise voltage source is denoted by  $G_{DCm}^U(X_0, \omega)$  under static conditions. By application of the quasi-stationary assumption [4] to each sideband, for the generic modulating function we find the expression

$$h_{k,m}^U(t, \omega) = \sqrt{\frac{G_{DCm}^U[x_{ss}(t), \omega + k\omega_0]}{G_{DCm}^U(X_0, \omega + k\omega_0)}} \quad (6)$$

Note that (5) are only valid for a set of fully correlated sources (or totally uncorrelated ones), because a diagonal matrix of modulating functions cannot correctly represent the independent modulation of correlation coefficients different from 1 or 0. The modulating functions (6) are independent of  $\omega$  when

$G_{DCm}^U(X_0, \omega)$  has the form  $G_{DCm}^U(X_0)F(\omega)$ .

Making use of (5), the sideband correlation matrices appearing in (3) may be written in the synthetic form

$$\begin{aligned} & \langle A_p(\omega) B_q^*(\omega) \rangle = \\ & = \sum_s H_{s,p-s}^A(\omega) \mathbb{C}_{DC}^{AB}(X_0, \omega + s\omega_0) H_{s,s-q}^B(\omega) \end{aligned} \quad (7)$$

where A, B stand for U, J in any possible combination, and  $\mathbb{C}_{DC}^{AB}(X_0, \omega)$  is the correlation matrix of the corresponding static noise sources. In the special but important case of sources of white noise, a generic entry (of subscripts i, j) of the correlation matrix (7) takes the simplified expression

$$\langle A_p B_q^* \rangle_{ij} = \mathbb{C}_{DCij}^{AB}(X_0) \mathbb{F}[h_i^A(t) h_j^B(t)]_{p,q} \quad (8)$$

where  $\mathbb{F}[\cdot]_s$  denotes the s-th harmonic of the periodic function of time enclosed in brackets. For white noise sources all the correlation matrices as well as the modulating functions are frequency independent, so that, for instance,  $h_{k,m}^A(t, \omega)$  reduces to  $h_m^A(t)$  for all  $k$ .

#### THE SCHOTTKY-BARRIER DIODE

Let us consider an epitaxial Schottky diode described as a nonlinear one-port depending on a state variable  $x(t)$ , physically identified as the voltage across the junction. The diode is modeled by the equivalent circuit of fig. 1, where  $i_F(x)$  represents the conduction current of the Schottky barrier. The linear contributions to the series resistance (e.g., the ohmic contacts) are included in the linear subnetwork, so that  $R_s(x)$  essentially accounts for the thickness changes of the undepleted epilayer. In the program  $i_F(x)$  is modeled by the usual exponential law, while  $C(x)$  and  $R_s(x)$  may be described by the standard Schottky-barrier laws or by arbitrary user-defined

functions. This allows different kinds of device structures to be treated in a unified way.

The noise sources  $i$  and  $u$  shown in fig. 1 account for the shot noise generated in the junction and for the noise generated in the undepleted epilayer, respectively. By inspection of fig. 1, the diode equivalent circuit can be redrawn as in fig. 2. In fig. 2 the two noise sources enclosed between the dashed lines have the same physical origin (shot noise), and are fully correlated. Their noise contribution is thus given by a summation of the form (3). The static correlation matrix is ( $e$  = electron charge)

$$\mathbb{C}_{DC}^{UJ(1)}(X_0) = 4\pi e \Delta f |i_F(X_0)| \begin{bmatrix} R_s^2(X_0) & R_s(X_0) \\ R_s(X_0) & 1 \end{bmatrix} \quad (9)$$

from which the modulating functions can be immediately obtained making use of (6). Since these sources are white, the correlations of their noise sidebands to be used in (3) are given by (8) and can be expressed as

$$\begin{aligned} \langle U_p U_q^* \rangle^{(1)} &= 4\pi e \Delta f \mathcal{F}[R_s^2\{x_{ss}(t)\} |i_F(x_{ss}(t))|]_{p,q} \\ \langle U_p J_q^* \rangle^{(1)} &= 4\pi e \Delta f \mathcal{F}[R_s\{x_{ss}(t)\} |i_F(x_{ss}(t))|]_{p,q} \\ \langle J_p J_q^* \rangle^{(1)} &= 4\pi e \Delta f \mathcal{F}[|i_F(x_{ss}(t))|]_{p,q} \end{aligned} \quad (10)$$

The noise voltage source  $u$  shown in fig. 2 accounts for the thermal noise generated in the series resistance and for various mechanisms of excess noise generation in the undepleted epilayer [7]. In the noise analysis it is thus treated as the series connection of several uncorrelated noise sources. The thermal contribution is expressed by the first term on the RHS of (3) with sideband correlations computed by (8) as

$$\langle U_p U_q^* \rangle^{(2)} = 4K_B T_0 \Delta f \mathcal{F}[R_s\{x_{ss}(t)\}]_{p,q} \quad (11)$$

where  $K_B$  is Boltzmann's constant and  $T_0$  is the physical temperature of the diode.

Excess noise is a complex phenomenon having a variety of physical origins [7]. In the following we shall assume that the dominant mechanisms are, i), hot electron generation combined with intervalley scattering, and, ii), the scattering of electrons by traps located in the undepleted epilayer and characterized by a single time constant  $\tau$ . The former contribution can be described by introducing an excess noise temperature of the series resistance,  $\Delta T(i_F)$ , whose dependence on current is qualitatively shown in fig. 3.  $\Delta T(i_F)$  is described by a third-order polynomial approximation of measured values (as in [7]) between two bounds  $I_{min}$ ,  $I_{max}$ , and is held constant outside this range. The static spectral density of this source may be written

$$G_{DC}^{U(3)}(X_0) = 4K_B \Delta f R_s(X_0) \Delta T[i_F(X_0)] \quad (12)$$

The corresponding noise contribution in dynamic conditions is thus given by the first term on the RHS of (3) with sideband correlations expressed by (8) as

$$\langle U_p U_q^* \rangle^{(3)} = 4K_B \Delta f \mathcal{F}[R_s\{x_{ss}(t)\} \Delta T[i_F(x_{ss}(t))]]_{p,q} \quad (13)$$

Finally, the static spectral density of the trap scattering noise may be written [7]

$$G_{DC}^{U(4)}(X_0, \omega) = \mathbb{C}_{DC}^{UU(4)}(X_0, \omega) = \alpha \frac{R_s(X_0) i_F^2(X_0)}{1 + (\omega \tau)^2} \quad (14)$$

where  $\alpha$  is an empirical constant. From (6) we obtain the modulating function

$$h^{U(4)}(t) = \frac{|i_F(x_{ss}(t))|}{|i_F(X_0)|} \sqrt{\frac{R_s(x_{ss}(t))}{R_s(X_0)}} \quad (15)$$

which is independent of  $\omega$ . The dynamic noise contribution is given by the first term on the RHS of (3), with the sideband correlations computed by (7) since this source is coloured:

$$\begin{aligned} \langle U_p(\omega) U_q^*(\omega) \rangle^{(4)} &= 2\pi \alpha \Delta f R_s(X_0) i_F^2(X_0) \cdot \\ &\cdot \sum_s \frac{H_{p-s}^{U(4)} H_{s-q}^{U(4)}}{1 + [(\omega + s\omega_0)\tau]^2} \end{aligned} \quad (16)$$

where  $H_k^{U(4)}$  is the  $k$ -th harmonic of (15). The above discussion extends the analysis presented by Crowe *et al.* [9] in a twofold way, that is, i), by taking into account the nonlinearity of the series resistance, and, ii), by taking into account the frequency-dependent trapping mechanism.

As an example of application, in fig. 5 we plot as a function of the local-oscillator power the computed noise temperature of a mm-wave diode mixer having the simple topology shown in fig. 4, and operated at 20 K. The diode parameters are assigned the typical values [10]  $I_S = 1.9 \cdot 10^{-52}$  A (saturation current), and  $C_{TO} = 8$  fF (zero-bias depletion-layer capacitance). The diode noise model is taken from [7], with parameters  $\Delta T(I_{max}) = 5000$  K,  $I_{min} = 0.1$  mA,  $I_{max} = 12$  mA,  $\alpha = 6.59 \cdot 10^{-15}$   $\Omega$ s,  $\tau = 66$  ps. Two IF values of 50 MHz and 5 GHz are considered, with a same LO frequency of 110 GHz. For each IF, the noise temperature is computed with and without excess noise, and with a linear and nonlinear series resistance (in the former case,  $R_s$  is set to  $R_s(0)$ ). Note the appearance of an optimum LO level when the full noise generation mechanism is accounted for [9]. With low IF values the same qualitative behavior is observed, but the contribution of the trapping noise becomes significant at high drive levels, and the noise temperature raises considerably. Note that for this kind of diode the effects of the series resistance nonlinearity are comparatively small. However, this would not be the case in other applications involving different types of diodes, such as planar Schottky varactors [11], which are known to exhibit large  $R_s$  changes as a function of bias.

The computation of the curves in fig. 5 took 136 seconds overall on a SUN SPARCstation 2 (31 power points per curve). Less than 16% of this time was spent in the noise analysis. This clearly demonstrates the high numerical efficiency of the noise analysis technique based on circuit decomposition.

#### ACKNOWLEDGMENTS

This work was partly sponsored by the Italian National Research Council (CNR) and by the Istituto Superiore delle Poste e delle Telecomunicazioni (ISPT).

## REFERENCES

- [1] C. Dragone, "Analysis of thermal and shot noise in pumped resistive diodes", *Bell Syst. Tech. J.*, Vol. 47, Nov. 1968, pp. 1883-1902.
- [2] D. N. Held and A. R. Kerr, "Conversion loss and noise of microwave and millimeter-wave mixers: part 1 - theory", *IEEE Trans. Microwave Theory Tech.*, Vol. MTT-26, Febr. 1978, pp. 49-55.
- [3] H. J. Siweris and B. Schiek, "A GaAs FET oscillator noise model with a periodically driven noise source", *Proc. 16th European Microwave Conf.* (Dublin), Sept. 1986, pp. 681-686.
- [4] V. Rizzoli and A. Neri, "State of the art and present trends in nonlinear microwave CAD techniques", *IEEE Trans. Microwave Theory Tech.*, Vol. 36, Feb. 1988, pp. 343-365.
- [5] S. Heinen, J. Kunisch, and I. Wolff, "A unified framework for computer-aided noise analysis of linear and nonlinear microwave circuits", *IEEE Trans. Microwave Theory Tech.*, Vol. 39, Dec. 1991.
- [6] A. Cappy, "Noise modeling and measurement techniques", *IEEE Trans. Microwave Theory Tech.*, Vol. 36, Jan. 1988, pp. 1-10.
- [7] A. Jelenski, E. L. Kollberg, and H. H. G. Zirath, "Broad-band noise mechanisms and noise measurements of metal-semiconductor junctions", *IEEE Trans. Microwave Theory Tech.*, Vol. MTT-34, Nov. 1986, pp. 1193-1201.
- [8] V. Rizzoli and A. Lipparini, "Computer-aided noise analysis of linear multiport networks of arbitrary topology", *IEEE Trans. Microwave Theory Tech.*, Vol. MTT-33, Dec. 1985, pp. 1507-1512.
- [9] T. W. Crowe and R. J. Mattauch, "Analysis and optimization of millimeter- and submillimeter- wavelength mixer diodes", *IEEE Trans. Microwave Theory Tech.*, Vol. MTT-35, Feb. 1987, pp. 159-168.
- [10] M. T. Faber and J. W. Archer, "Millimeter-wave, shot-noise limited, fixed-tuned mixer", *IEEE Trans. Microwave Theory Tech.*, Vol. MTT-33, Nov. 1985, pp. 1172-1178.
- [11] P. Philippe, W. El-Kamali, and V. Pauker, "Physical equivalent circuit model for planar Schottky varactor diode", *IEEE Trans. Microwave Theory Tech.*, Vol. 36, Feb. 1988, pp. 250-255.

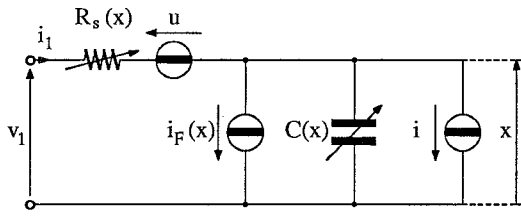


Fig. 1 - Equivalent circuit of a noisy diode.

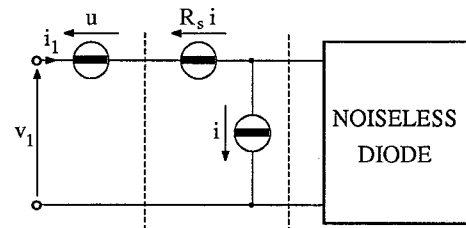


Fig. 2 - Equivalent transformation of the topology in fig. 1.

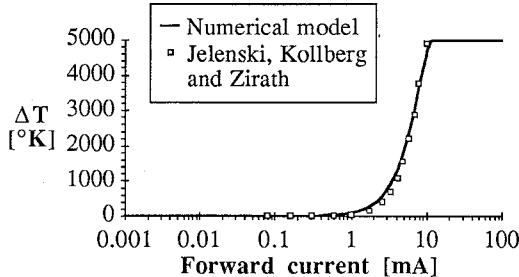


Fig. 3 - Overtemperature due to hot electrons and intervalley scattering.

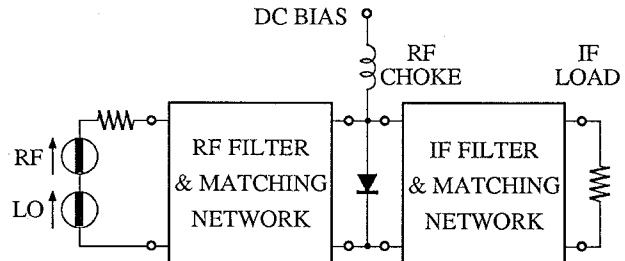


Fig. 4 - Schematic of a mm-wave mixer.

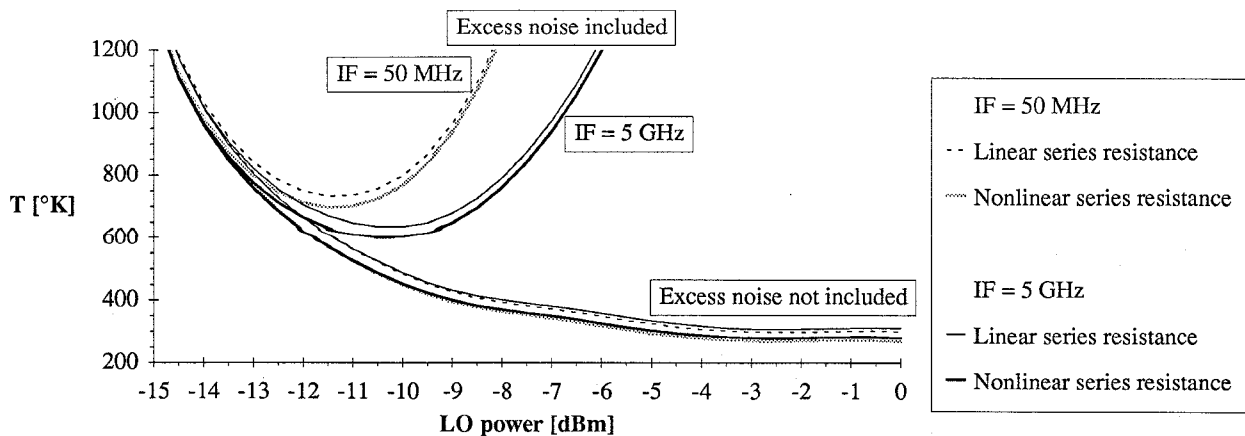


Fig. 5 - Noise temperature of a mm-wave mixer.